

Calculations of high energy particle losses for Uragan-2M taking into account the influence of current-feeds and detachable joints of the helical winding *

V. V. Nemov^{1,2}, S. V. Kasilov^{1,2}, W. Kernbichler², V. N. Kalyuzhnyj¹, B. Seiwald²

¹ Institute of Plasma Physics, National Science Center “Kharkov Institute of Physics and Technology”, Akademicheskaya Str. 1, 61108 Kharkov, Ukraine

² Association EURATOM-ÖAW, Institut für Theoretische Physik - Computational Physics, TU Graz, Petersgasse 16, A-8010 Graz, Austria

Introduction

A study of collisionless charged particle losses (in particular, α -particle losses) is important for assessment of general confinement properties of stellarator devices. For the presented numerical studies for magnetic configurations of U-2M (Uragan-2M [1], $l=2$ torsatron, $R_0=170$ cm, $n_p=4$, R_0 is the big radius of the torus, n_p is the number of the helical field periods along the torus) the influence of current-feeds and detachable joints of the helical winding are taken into account. Because of the non-symmetric arrangement of the indicated elements of the magnetic system the stellarator symmetry of the resulting magnetic field of U-2M is broken. This requires a special approach for the computation of the gradient of the magnetic surface function, $\nabla\psi$, which is necessary for the numerical particle confinement study. Such an approach has been elaborated recently in [2].

To assess particle losses the technique proposed in [3,4] is combined with the technique of [2] for the computation of $\nabla\psi$. For the calculation of the magnetic field the Biot-Savart code, presented in [5], as well as the Lagrange polynomial interpolation are used.

Initial conditions

To evaluate losses of charged particles, target functions which have been introduced in [3,4] and further denoted as Γ_v , Γ_w , Γ_{wp} and Γ_c are used. These functions have been obtained using the mean-square average over the pitch angle and over the magnetic surface of the bounce-averaged ∇B drift velocity of trapped particles across magnetic surfaces and in the poloidal direction. For the normalization of all drift velocities the quantity $v\rho_L/R_0$, where ρ_L is the characteristic Larmor radius and v is the absolute value of the particle velocity, is used. In this case Γ_v represents the average of the bounce-averaged ∇B drift velocity of trapped particles across a magnetic surface, Γ_w corresponds to an integral effect of the square of the ∇B drift, Γ_{wp} corresponds to an integral effect of the square of the poloidal drift, and Γ_c corresponds to an integral value of the square of the angle between the J_{\parallel} contour and the magnetic surface. All these factors are dimensionless.

*This work, supported by the European Communities under the contract of Association between EURATOM and the Austrian Academy of Sciences, was carried out within the framework of the European Fusion Development Agreement. The views and opinions expressed herein do not necessarily reflect those of the European Commission. Additional funding is provided by the Austrian Science Foundation, FWF, under contract number P16797-N08.

For a specific configuration each of these factors is only a function of the minor radius of the magnetic surface. In general, a decrease of Γ_v , Γ_w and Γ_c corresponds to a reduction of the radial drift velocity of the trapped particles which is important for stellarator optimization. On the other hand an increase of Γ_{wp} is desirable since this corresponds to an enhancement of the velocity of the poloidal motion of trapped particles which promotes the formation of closed contours of J_{\parallel} . Among the four dimensionless quantities the parameter Γ_c turns out to be the most important. This parameter is obtained by a combined study of the radial as well as the poloidal drifts of trapped particles and allows to assess the measure of closeness of contours of J_{\parallel} (see [4]).

Studies for two different magnetic configurations of U-2M are presented. For both configurations magnetic field parameters are chosen to provide magnetic surfaces which are well centered with respect to the vacuum chamber. For the first configuration the toroidal magnetic field is chosen in such a way that the rotational transform ι is within $1/3 < \iota < 1/2$ ($k_{\varphi}=0.31$, see, in [1,5]). The second configuration ($k_{\varphi}=0.295$, see [1]) has a slightly larger toroidal magnetic field and ι within $0.31 < \iota < 0.383$. For this configuration the resonant magnetic surfaces with $\iota = 1/3$ are inside the confinement region.

For calculating the magnetic field and its spatial derivatives the Biot-Savart code, which has been developed in [5], is used. Current-feeds and detachable joints of the helical winding are taken into account. For comparison, supplemental computations are performed for the magnetic field calculated using the Lagrange polynomial interpolation on a three dimensional grid. The grid data are obtained in preliminary Biot-Savart computations.

Computational results

Using the corresponding formulas of [3,4] the above mentioned Γ factors as well as $\nabla\psi$ can be calculated in real-space and in magnetic coordinates with help of a field line following code. For the evaluation of the Γ factors connected with the poloidal motion of the trapped particles, Γ_c and Γ_{wp} , respectively, the radial electric field is assumed to be zero because of its negligible effect on α -particle motion. The computational results are presented in Figs.1-4 as functions of r/a , with r being the mean radius of a given magnetic surface and a being the mean radius of the outermost magnetic surface inside the vacuum chamber. Each figure shows results corresponding to the magnetic field using the Biot-Savart code of [5] (lines with points) as well as the Lagrange polynomial interpolation (points). It follows from the figures that the results obtained with both techniques are in good agreement to each other. Additionally, also results without the influence of current-feeds and detachable joints of the helical winding are present in each figure (solid lines).

The influence of the current-feeds and detachable joints of the helical winding leads to a formation of island magnetic surfaces of significant sizes. These surfaces correspond to rational values of the rotational transform ι of $\iota=2/5$ for $k_{\varphi}=0.31$ and of $\iota = 1/3$ for $k_{\varphi}=0.295$. In terms of r/a these island regions correspond schematically to r/a of $0.87 < r/a < 0.96$ for $k_{\varphi}=0.31$ and $0.61 < r/a < 0.85$ for $k_{\varphi}=0.295$. For these island surfaces the values of Γ_v and Γ_w are enhanced compared to the values for the adjacent non-island surfaces. The influence of the current-feeds

and detachable joints leads to irregularities of Γ_c and Γ_{wp} which manifest itself in an increase of Γ_{wp} and a decrease of Γ_c in the island regions $\iota=2/5$ (for $k_\varphi=0.31$) and $\iota=1/3$ (for $k_\varphi=0.295$). A similar behavior of Γ_{wp} and Γ_c can be seen also in the vicinity of these island surfaces and for the regions between the indicated islands and the boundary surfaces. These irregularities are a consequence of magnetic islands of smaller sizes (e.g., in case of $k_\varphi=0.295$ they take place for $\iota=6/17$ ($r/a \approx 0.868$), $\iota=5/14$ ($r/a \approx 0.89$), $\iota=4/11$ ($r/a \approx 0.92$), $\iota=3/8$ ($r/a \approx 0.97$), and $\iota=14/37$ ($r/a \approx 0.985$)). An increase of Γ_{wp} correlates with a decrease of Γ_c .

When the influence of current-feeds and detachable joints of the helical winding is neglected, the above mentioned irregularities in graphs of Γ_v and Γ_w are not seen. However, narrow regions of r/a are present for which Γ_{wp} is somewhat higher and Γ_c is somewhat lower than for the adjacent magnetic surfaces. This takes place for $r/a \approx 0.9$ in the vicinity of resonant magnetic surfaces of $\iota=2/5$ in case of $k_\varphi=0.31$ as well as for $r/a \approx 0.71$ and $r/a \approx 0.91$ in the vicinity of resonant magnetic surfaces of $\iota=1/3$ and $\iota=4/11$, respectively, for the configuration with $k_\varphi=0.295$.

In Figs. 3 and 4 an additional factor Γ_{cm} is presented. This factor represents, in arbitrary units, the phase volume occupied by trapped particles (see in [4]). For a classical stellarator with large aspect ratio it can be evaluated as $\sqrt{\varepsilon_h}$, with ε_h being the helical ripple of the magnetic field.

It is of interest to compare the obtained results with the analogous results obtained in [4] for different stellarator configurations. For the CHS configuration which is characteristic for a small aspect ratio heliotron-torsatron devices, Γ_c is of the same order as obtained for U-2M. At the same time for the drift orbit optimized (inward shifted) CHS configuration, Γ_c is 3 \div 5 times smaller. The maximum decrease for Γ_c is realized for the quasi-isodynamical configuration for which Γ_c is 10 \div 50 times smaller than the obtained values for U-2M.

Summary

Target functions which have been introduced in [3,4] are used to assess of trapped particle confinement for two characteristic magnetic configurations of U-2M. For the first configuration the rotational transform ι is within the limits $1/3 < \iota < 1/2$ ($k_\varphi=0.31$, see in [1]) and for the second $0.31 < \iota < 0.383$ ($k_\varphi=0.295$). The computations are performed in real-space coordinates using the field line following codes. The influences of current-feeds and detachable joints of the helical winding cause considerable island magnetic surfaces arising for $\iota=2/5$ ($k_\varphi=0.31$) as well as for $\iota=1/3$ ($k_\varphi=0.295$). For these island magnetic surfaces and in their vicinity particle confinement is improved. This improvement can be explained by an increased velocity of the poloidal drift of trapped particles in these regions. The measure of the closure of contours of J_{\parallel} for U-2M is of the same order as for the CHS standard configuration. At the same time for the drift orbit optimized CHS configuration (inward shifted) this measure is significantly better than for U-2M.

References

[1] O. S. Pavlichenko for the U-2M group, First results from the "URAGAN-2M" torsatron, *Plasma Phys. Control. Fusion* **35**, B223-B230 (1993).

- [2] V. V. Nemov et al., Proc. 36th EPS Conf. on Plasma Phys. Sofia, June 29-July 3, 2009, ECA Vol.33E, P-4.127 (2009)
- [3] V. V. Nemov et al., Phys. Plasmas, **12**, 112507 (2005)
- [4] V. V. Nemov et al., Phys. Plasmas, **15**, 052501 (2008)
- [5] V. V. Nemov et al., Proc. 34th EPS Conf. on Plasma Phys., Warsaw, Poland, 2-6 July 2007, ECA Vol.31F, P-1.077 (2007)

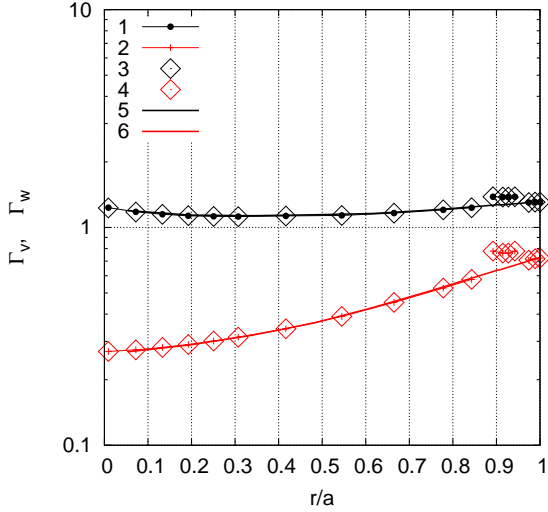


Fig.1. Factors Γ_v (graphs 1, 3 and 5) and Γ_w (graphs 2, 4 and 6) for $k_\varphi=0.31$; graphs 1 and 2 correspond to the Biot-Savart code, graphs 3 and 4 correspond to the Lagrange polynomial interpolation, for the graphs 5 and 6 current-feeds and detachable joints of the helical winding are not taken into account.

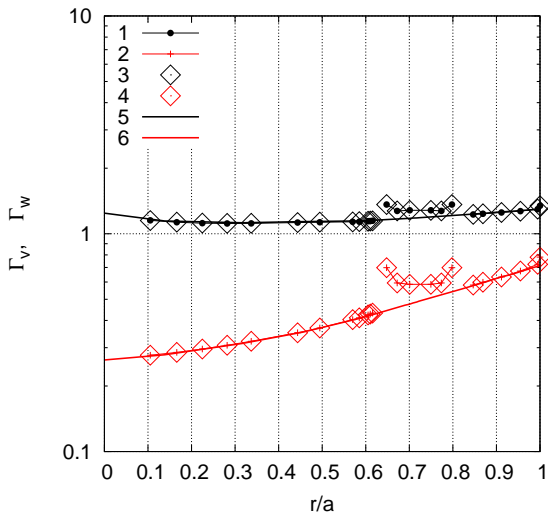


Fig.2. The same as in Fig. 1 for $k_\varphi=0.295$.

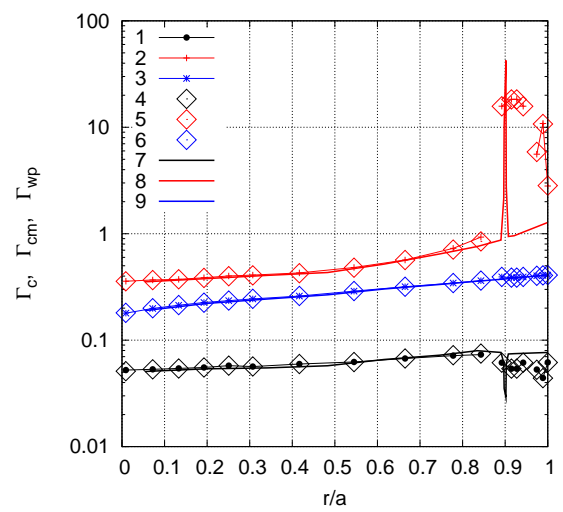


Fig.3. Factors Γ_c (graphs 1, 4 and 7), Γ_{wp} (graphs 2, 5 and 8) and Γ_{cm} (graphs 3, 6 and 9) for $k_\varphi=0.31$; graphs 1, 2 and 3 correspond to the Biot-Savart code, graphs 4, 5 and 6 correspond to the Lagrange polynomial interpolation, for the graphs 7, 8 and 9 current-feeds and detachable joints of the helical winding are not taken into account.

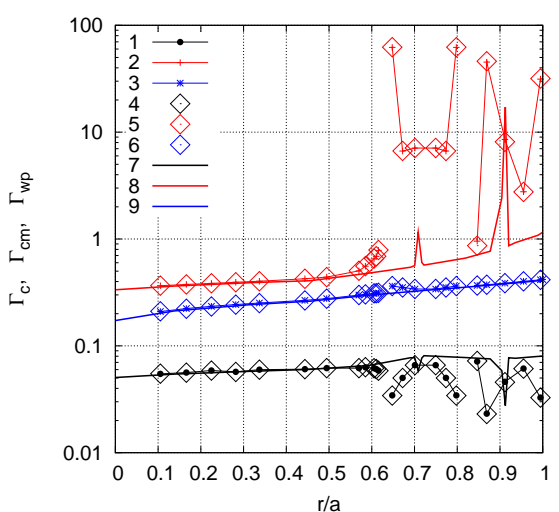


Fig.4. The same as in Fig. 3 for $k_\varphi=0.295$.